Asian Journal of Chemistry; Vol. 28, No. 6 (2016), 1244-1252

ASIAN JOURNAL OF CHEMISTRY

http://dx.doi.org/10.14233/ajchem.2016.19641

DFT Studies of Synthesis of (4R,5S,8as)-4,5,8a-Triphenylhexahydropyrimido[4,5-d]pyrimidine-2,7(1*H*,3*H*)-dione

QI-SHAN HU[1,*], YUN-QING HE[2] and LAI-CAI LI[3]

[1]College of Chemistry and Chemical Engineering, Sichuan University of Arts and Science, Dazhou 635711, P.R. China
[2]College of Chemistry, Leshan Normal University, Leshan 614000, P.R. China
[3]College of Chemistry and Material Science, Sichuan Normal University, Chengdu 610066, P.R. China

*Corresponding author: E-mail: huqs@163.com

Received: 29 September 2015; *Accepted*: 21 December 2015; *Published online*: 29 February 2016; AJC-17784

The mechanism of one-pot reaction of benzaldehyde, urea and acetophenone for the synthesis of (4R,5S,8as)-4,5,8a-triphenylhexahydropyrimido[4,5-d]pyrimidine-2,7(1*H*,3*H*)-dione catalyzed by protonic acid was investigated by density functional theory (DFT). The geometries and the frequencies of reactants, intermediates, transition states and products were calculated at the B3LYP/6-311G(d) level. The vibration analysis and the IRC analysis verified the authenticity of transition states. The reaction processes were confirmed by the changes of charge density at the bond-forming critical point. The results indicated that protonic acid is an effective catalyst in the synthesis of (4R,5S,8as)-4,5,8a-triphenylhexahydropyrimido[4,5-d]pyrimidine-2,7(1*H*,3*H*)-dione from benzaldehyde, urea and acetophenone. The activation energy of reaction with protonic acid decreased by 104.3 kJ mol^{-1} compared with that of the reaction without it. The mechanism of reaction with catalyst protonic acid differs from that of reaction without it.

Keywords: Density functional theory, Biginelli reaction, Dihydropyrimidone.

INTRODUCTION

In recent years, the Biginelli reaction is extensively used to the organic synthesis [1-12]. The Biginelli-type compound dihydropyrimidones show an attractive pharmacological profile as calcium channel blockers, antihypertensive agents, α-A-antagonists and neuropeptide Y (NPY) antagonists [13-18]. One-pot synthesis method is used to synthesize the dihydropyrimidones and their derivatives [19-20]. (4R,5S,8as)-4,5,8a-triphenylhexahydropyrimido[4,5-d]pyrimidine-2,7(1*H*,3*H*)-dione in from multi-component condensation of benzaldehyde, urea and acetophenone [21]. In the literature [21], the Biginelli reaction of ethyl acetoacetate, an aromatic aldehyde and urea could be efficiently catalyzed by potassium hydrogen sulfate in glycol and the desired product was obtained in high yield. There is no literature about the mechanism of synthesis of (4R,5S,8as)-4,5,8a-triphenylhexahydropyrimido-[4,5-d]pyrimidine-2,7(1*H*,3*H*)-dione. Atoms in molecules (AIM) analysis was studied for the reaction mechanism synthesis of (4R,5S,8as)-4,5,8a-triphenylhexahydropyrimido[4,5-d]-pyrimidine-2,7(1*H*,3*H*)-dione. The quantum theory of atoms in molecules (QTAIM) is a model of molecular and condensed matter electronic systems (such as crystals) in which the principal objects of molecular structure - atoms and bonds - are natural expressions of a system's observable electron density distribution function. An electron density distribution of a molecule is a probability distribution that describes the average manner in which the electronic charge is distributed throughout real space in the attractive field exerted by the nuclei. It is extensively used to research of the reaction mechanism [22,23]. The main purposes of this paper are as follows: (1) to investigate the microscopic mechanism of reaction among benzaldehyde, urea and acetophenone for the synthesis of (4R,5S,8as)-4,5,8a-triphenylhexahydropyrimido[4,5-d]pyrimidine-2,7(1*H*,3*H*)-dione catalyzed by protonic acid by way of density functional theory (DFT). (2) to confirm the rate-determining step of the reaction.

COMPUTATIONAL METHODS

The mechanism of reaction among benzaldehyde, urea and acetophenone for the synthesis of (4R,5S,8as)-4,5,8a-triphenylhexahydropyrimido[4,5-d]pyrimidine-2,7(1*H*,3*H*)-dione was investigated catalyzed by protonic acid by way of density functional theory (DFT). The geometries and the frequencies of reactants, intermediates, transition states and products were calculated at the B3LYP/6-311G(d) level [24]. Stable structures were obtained. The parameters of geometry configuration are shown in Fig. 1 (R1-P2) and Fig. 2 (R1B-IM3D2). The vibration analysis and the IRC analysis proved the authenticity of intermediates and transition states. The

reaction processes were confirmed by the changes of charge density at the bond-forming critical point (as shown by the numeric value in the parentheses in Figs. 1 and 2). All calculations were carried out with the Gaussian 03 program [25].

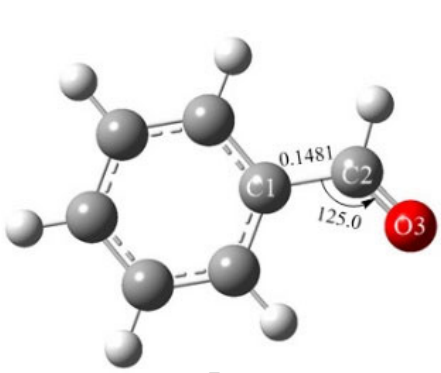

R1

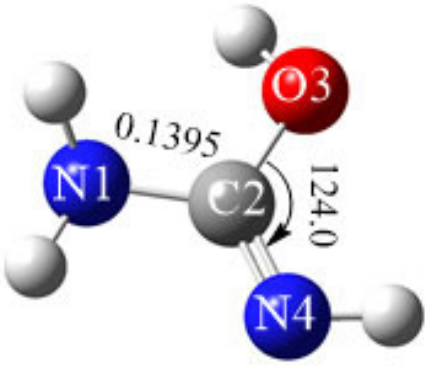

R2B

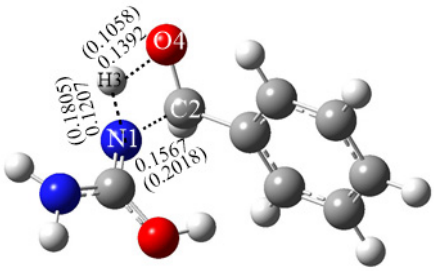

TS1A

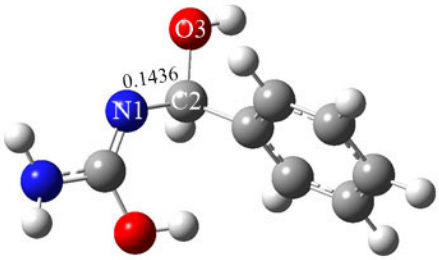

IM1A

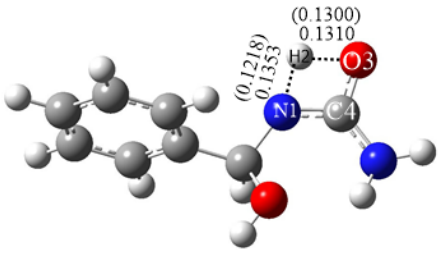

TS1B

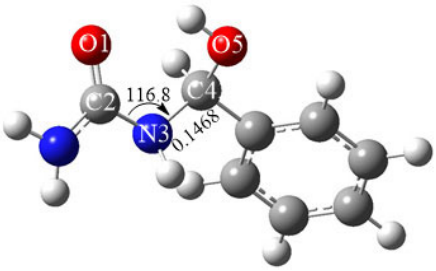

IM1B

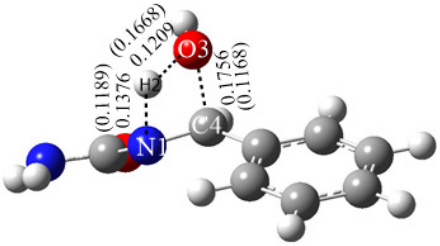

TS1C

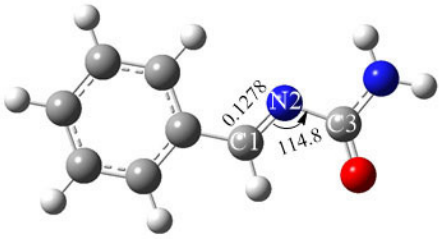

IM1C

P1

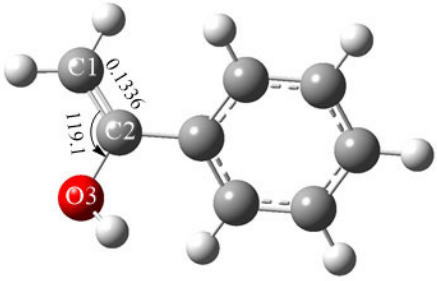

R3B

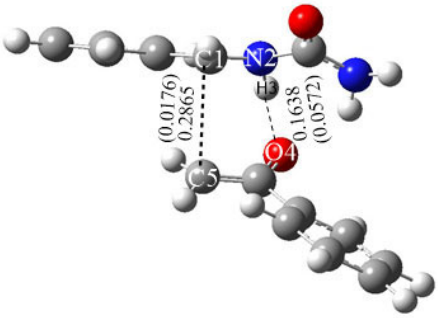

TS2A

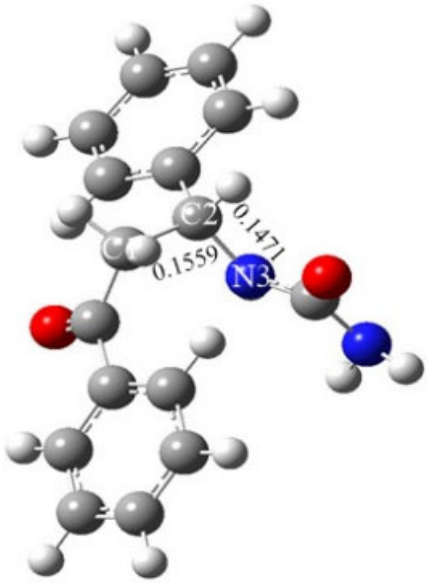

IM2A

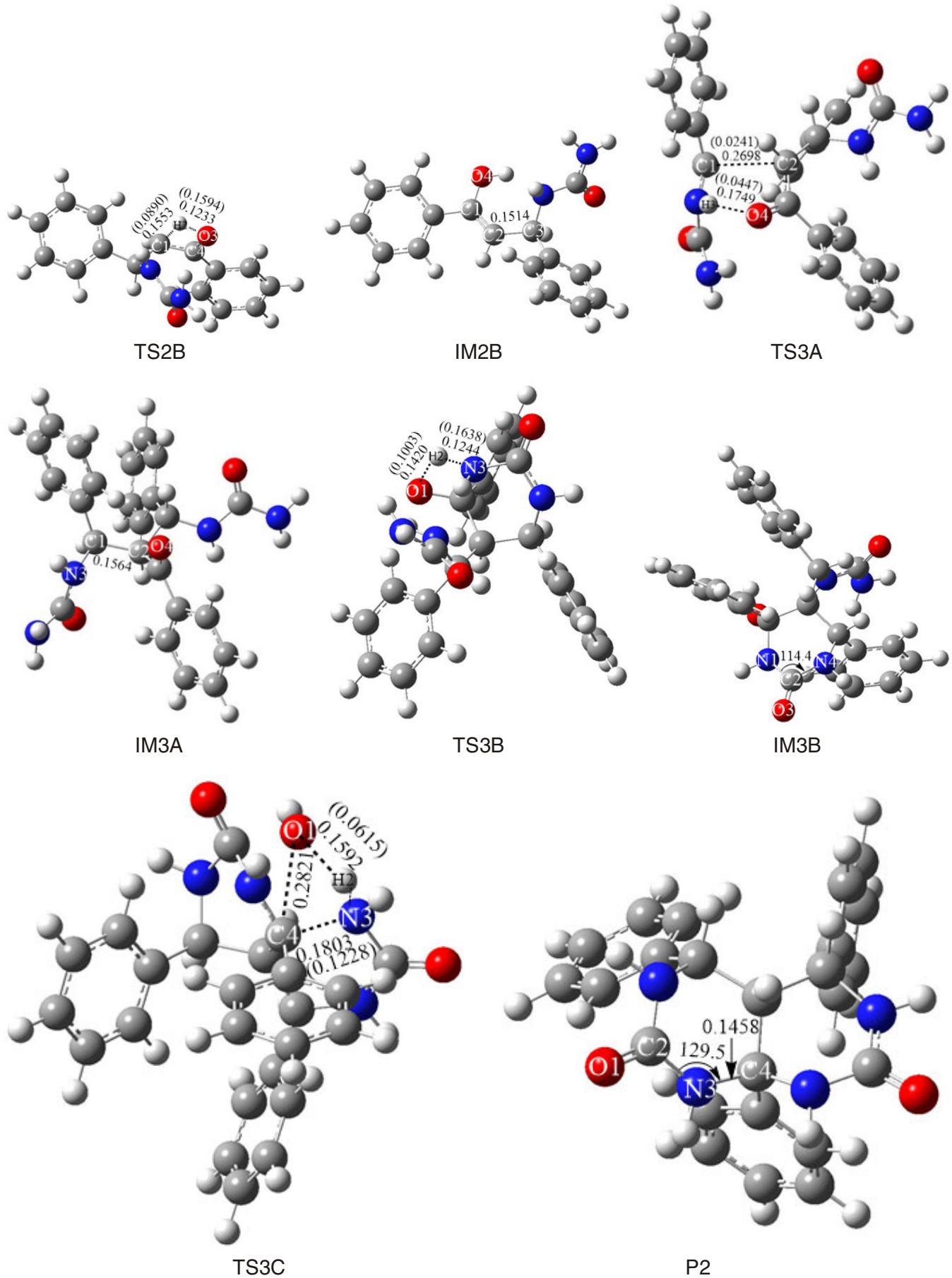

Fig. 1. Optimized geometric configurations of various compounds in the reaction: bond length in nanometers, bond angle in degree, charge density at bond-forming critical point in a.u.

RESULTS AND DISCUSSION

The calculated energies (E) and relative energies (E_{rel}) of reactants, intermediates, transition states and products are listed in Table-1. All energies (E) include zero-point energy (ZPE) corrections. Vibration frequencies of reactants, intermediates and products are positive and those of all transition states have only one imaginary frequency. Fig. 3 is a schematic map of energy levels for the reaction without protonic acid and with protonic acid.

Reaction mechanism and energy analysis of the reaction without protonic acid: The reaction between R1 and R2B for the synthesis of IM1A is a nucleophilic reaction. Firstly, the N4 atom of R2B attacks the carbonyl carbon atom of benzaldehyde to form intermediate IM1A through transition state TS1A. In TS1A, the bond length and the charge density

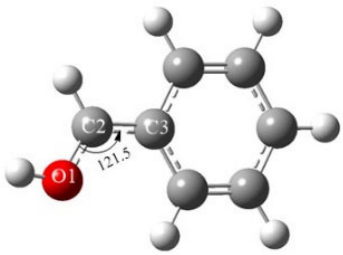

R1B

R4

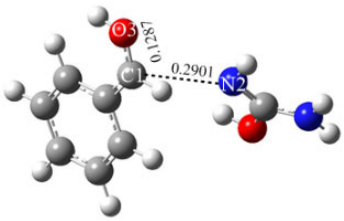

TS1A2

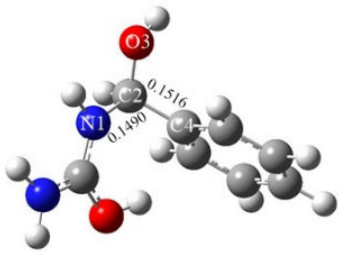

IM1A2

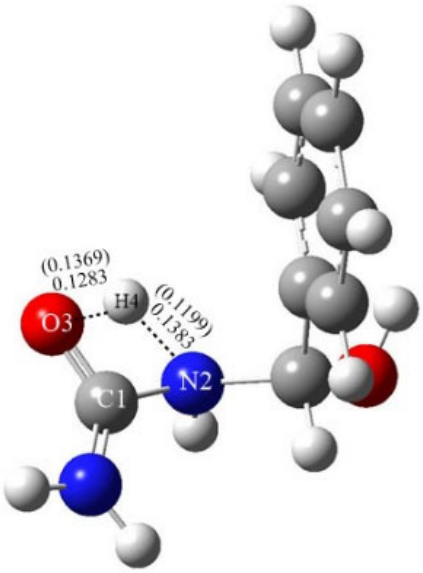

TS1B2

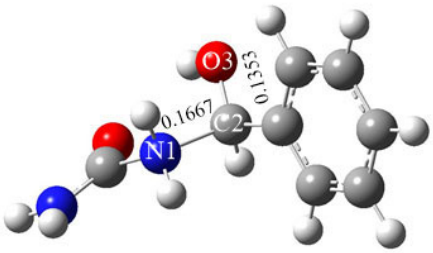

IM1B2

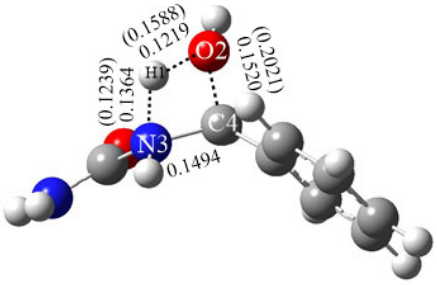

TS1C2

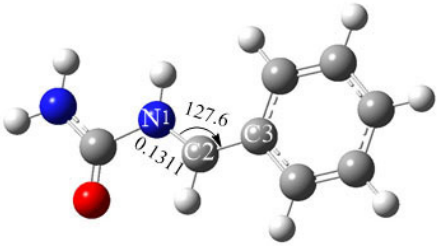

IM1C2

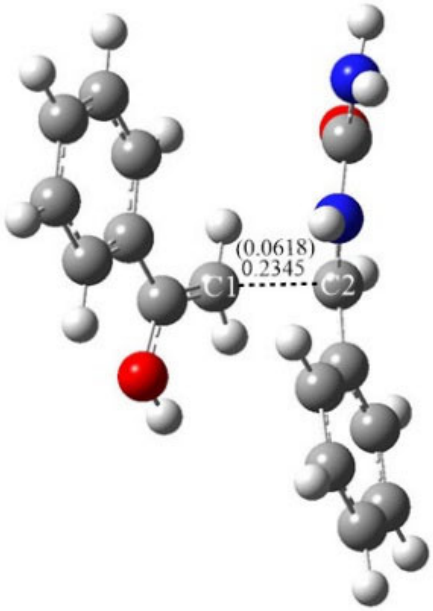

TS2A2

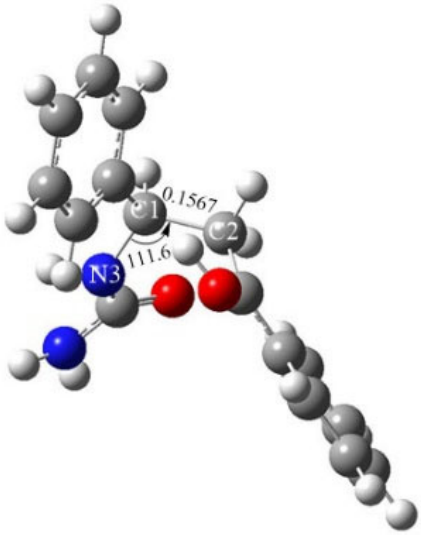

IM2A2

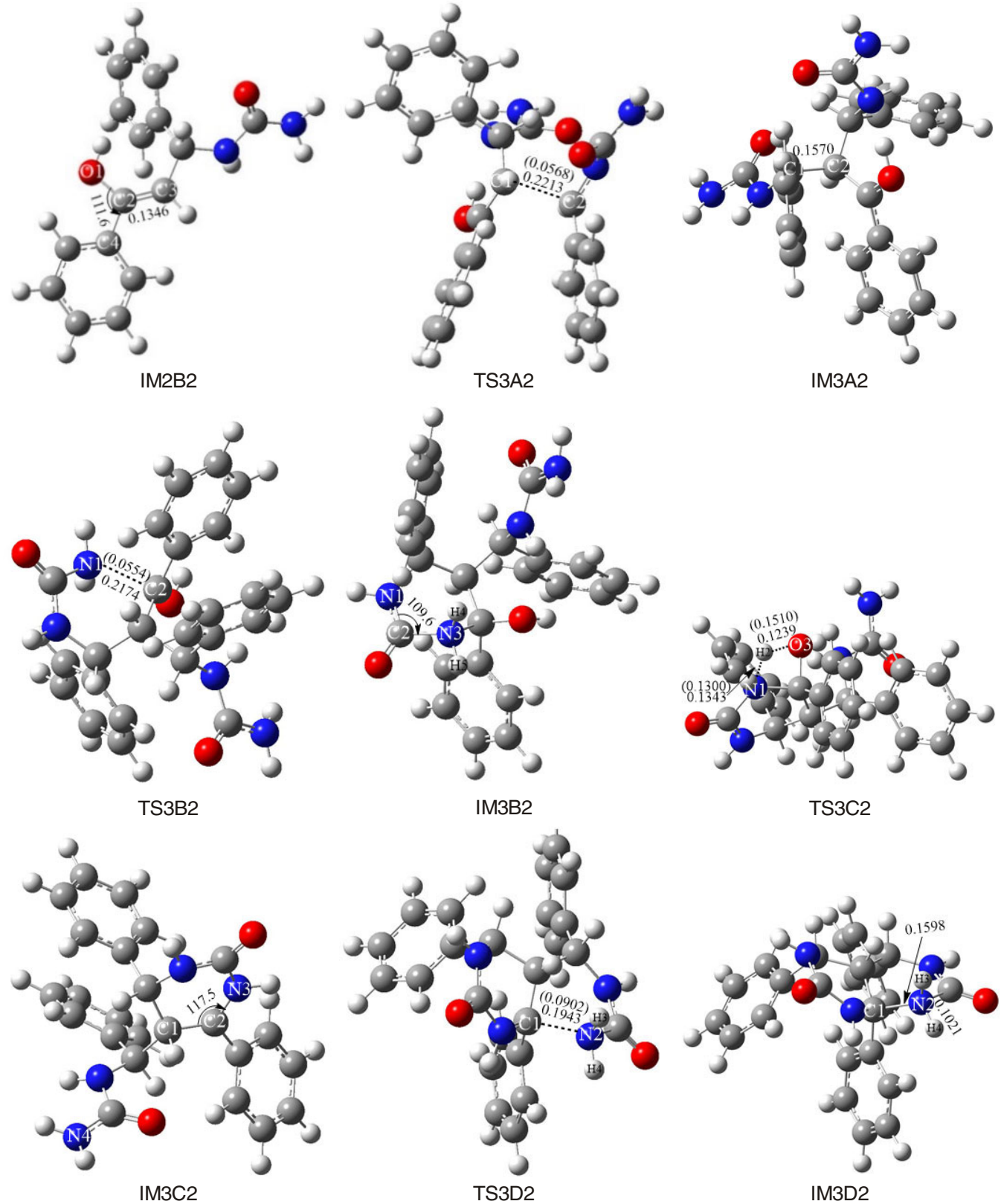

Fig. 2. Optimized geometric configurations of various compounds in the reaction: bond length in nanometers, bond angle in degree, charge density at bond-forming critical point in a.u.

at bond-forming critical point of N1–C2, N1-H3 and H3-O4 are 0.1567 nm and 0.2018 a.u., 0.1207 nm and 0.1805 a.u. and 0.1392 nm and 0.1058 a.u., respectively and the activation energy is 146.29 kJ mol^{-1}. IM1A forms intermediate IM1B through transition state TS1B. This is a hydrogen atom transfer process. In TS1B, the bond length and the charge density at the bond-forming critical point of N1-H2 are 0.1353 nm and 0.1218 a.u., respectively and those of H2–O3 are 0.1310 nm and 0.1300 a.u., respectively and the activation energy is 87.33 kJ mol^{-1}. The IM1B forms the IM1C and P1 through transition

TABLE-1
ENERGIES (E) AND RELATIVE ENERGIES (E_{rel}) OF VARIOUS SPECIES AND IMAGINARY FREQUENCY OF TRANSITIONS

Species	-E (a.u.)	E_{rel} (kJ mol^{-1})	ν (cm^{-1})
R1' (2R1 + 2R2B + R3B)	1526.35379	0	
TS1A' (R1 + R2B + TS1A + R3B)	1526.29807	146.29	-1616.1
IM1A' (R1 + R2B + IM1A + R3B)	1526.34833	14.33	
TS1B' (R1 + R2B + TS1B + R3B)	1526.31507	101.66	-1919.08
IM1B' (R1 + R2B + IM1B + R3B)	1526.39074	-97.01	
TS1C' (R1 + R2B + TS1C + R3B)	1526.30962	115.98	-1799.54
IM1C' (R1 + R2B + IM1C + R3B + P1)	1526.37167	-46.95	
TS2A' (R1 + R2B + TS2A + P1)	1526.35268	2.91	-132.94
IM2A' (R1 + R2B + IM2A + P1)	1526.40561	-136.05	
TS2B' (R1 + R2B + TS2B + P1)	1526.30287	133.70	-2118.11
IM2B' (IM1C + IM2B + 2P1)	1526.40662	-138.71	
TS3A' (TS3A + 2P1)	1526.36789	-37.00	-122.55
IM3A' (IM3A + 2P1)	1526.42753	-193.61	
TS3B' (TS3B + 2P1)	1526.33286	54.95	-1732.68
IM3B' (IM3B + 2P1)	1526.40658	-138.60	
TS3C' (TS3C + 2P1)	1526.29780	147.01	-291.48
P2A' (P2 + 3P1)	1526.37712	-61.20	
R1' (2R1 + 2R2B + R3B + 2R4)	1526.35379	0	
R1B' (2R1B + 2R2B + R3B)	1527.06679	-1864.85	
TS1A2' (R1B + R2B + TS1A2 + R3B)	1527.01039	-1717.34	-83.53
IM1A2' (R1B + R2B + IM1A2 + R3B)	1527.04685	-1812.69	
TS1B2' (R1B + R2B + TS1B2 + R3B)	1526.97755	-1631.43	-1851.91
IM1B2' (R1B + R2B + IM1B2 + R3B)	1527.03726	-1787.62	
TS1C2' (R1B + R2B + TS1C2 + R3B)	1526.99406	-1674.63	-1652.05
IM1C2' (R1B + R2B + IM1C2 + R3B + P1)	1527.06814	-1868.37	
TS2A2' (R1B + R2B + TS2A2 + P1)	1527.05418	-1831.86	-141.59
IM2A2' (R1B + R2B + IM2A2 + P1)	1527.07002	-1873.30	
IM2B2' (R1B + R2B + IM2C2 + 2P1)	1526.78018	-1115.24	
TS3A2' (TS3A2 + R4 + 2P1)	1526.77693	-1106.71	-233.19
IM3A2' (IM3A2 + R4 + 2P1)	1526.78803	-1135.77	
TS3B2' (TS3B2 + R4 + 2P1)	1526.74089	-1012.46	-108.21
IM3B2' (IM3B2 + R4 + 2P1)	1526.74735	-1029.35	
TS3C2' (TS3C2 + R4 + 2P1)	1526.71417	-942.57	-1729.75
IM3C2' (IM3C2 + R4 + 2P1)	1526.76180	-1067.15	
TS3D2' (TS3D2 + R4 + 3P1)	1526.71600	-947.58	-208.88
IM3D2' (IM3D2 + R4 + 3P1)	1526.71810	-952.84	
P2B' (P2 + 3P1 + 2R4)	1526.37712	-61.0	

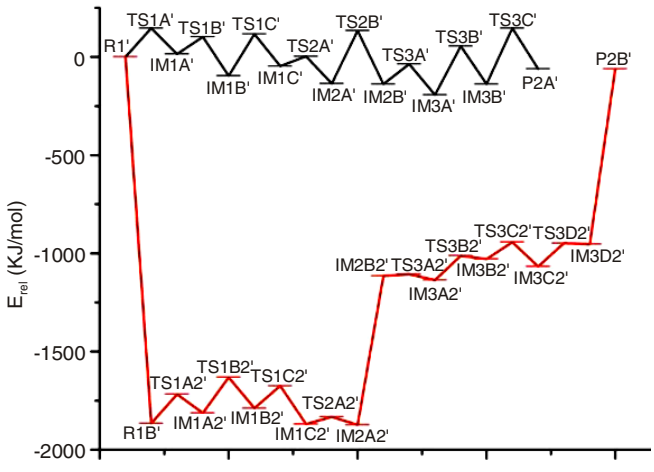

Fig. 3. Schematic map of energy levels in the reaction

state TS1C. This is a dehydration process. In TS1C, the bond length and the charge density at bond-forming critical point of N1–H2, H2-O3 and O3-C4 are 0.1376 nm and 0.1189 a.u., 0.1209 nm and 0.1668 a.u. and 0.1756 nm and 0.1168 a.u., respectively and the activation energy is 212.99 kJ mol^{-1}. The mechanism of the reaction is: R1 + R2B → TS1A → IM1A → TS1B → IM1B → TS1C → IM1C + H_2O

IM1C reacts with R3B to form intermediate IM2A through transition state TS2A. This is a concerted reaction processes with the forming bond of C1-C5 and the transfer of a hydrogen atom. A hydrogen atom of hydroxyl of R3B is transferred to nitrogen atom of IM1C in this processes. In TS2A, the bond length and the charge density at bond-forming critical point of C1–C5 are 0.2865 nm and 0.0176 a.u., respectively and those of H3–O4 are 0.1638 nm and 0.0572 a.u., respectively and the activation energy is 49.86 kJ mol^{-1}. IM2A then forms intermediate IM2B through transition state TS2B and this is a hydrogen atom transfer processes. In TS2B, the bond length and the charge density at bond-forming critical point of C1–H2 are 0.1553 nm and 0.0890 a.u., respectively and those of H2-O3 are 0.1223 nm and 0.1594 a.u., respectively and the activation energy is 269.75 kJ mol^{-1}. The mechanism of the reaction is: IM1C + R3B → TS2A → IM2A → TS2B → IM2B.

IM2B reacts with IM1C to form intermediate IM3A through transition state TS3A. This is also a concerted reaction process with the forming bond of C1-C2 and the transfer of a hydrogen atom. A hydrogen atom of hydroxyl of IM2B is

transferred to nitrogen atom of IM1C in this processes. In TS3A, the bond length and the charge density at bond-forming critical point of C1–C2 are 0.2698 nm and 0.0241 a.u., respectively and those of H3–O4 are 0.1749 nm and 0.0447 a.u., respectively and the activation energy is 101.71 kJ mol^{-1}. IM3A then forms intermediate IM3B through transition state TS3B. This is a concerted reaction process with the closing a ring and the transfer of a hydrogen atom. In TS3B, the bond length and the charge density at bond-forming critical point of O1–H2 are 0.1420 nm and 0.1003 a.u., respectively and those of H2–N3 are 0.1244 nm and 0.1638 a.u., respectively and the activation energy is 248.56 kJ mol^{-1}. IM3B then forms P1 and P2 through transition state TS3C. This is a concerted reaction process with the closing a ring and dehydration process. In TS3C, the bond length and the charge density at bond-forming critical point of N3–C4, C4-O1 and O1-H2 are 0.1803 nm and 0.1228 a.u., 0.2821 nm and 0.1592nm and 0.0615 a.u., respectively and the activation energy is 285.60 kJ mol^{-1}. This is a rate-determining step. The mechanism of the reaction is: IM2B + IM1C → TS3A → IM3A → TS3B → IM3B → TS3C → P2 + H_2O.

The overall reaction is: 2R1+2R2B+R3B → P2+3H_2O and the activation energy of the reaction is 285.60 kJ mol^{-1}.

The details of the reaction mechanism of the reaction are shown as Fig. 4.

Reaction mechanism and energy analysis of the reaction with catalyst protonic acid: Firstly, R1 reacts with hydrogen proton to form R1B. R1B reacts with R2B to form IM1A2 through transition state TS1A2. In TS1A2, the bond length of C1-N2 is 0.2901 nm, the activation energy is 147.50 kJ mol^{-1}. IM1A2 then forms intermediate IM1B2 through transition state TS1B2. This is a hydrogen atom transfer processes. In TS1B2, the bond length and the charge density at the bond-forming critical point of O3-H4 are 0.1283 nm and 0.1369 a.u., respectively and those of H4–N2 are 0.1383 nm and 0.1199 a.u., respectively and the activation energy is 181.26 kJ mol^{-1}. This is a rate-determining step. IM1B2 forms intermediate IM1C2 through transition state TS1C2. This is a dehydration processes. In TS1C2, the bond length and the charge density at bond-forming critical point of H1–O2, O2-C4 and N3-H1 are 0.1219 nm and 0.1588 a.u., 0.1520 nm and 0.2021 a.u. and 0.1364 nm and 0.1239 a.u., respectively and the activation energy is 112.99 kJ mol^{-1}. The mechanism of the reaction is: R1 + H^+ → R1B; R1B + R2B → TS1A2 → IM1A2 → TS1B2 → IM1B2 → TS1C2 + H_2O.

IM1C2 reacts with R3B to form IM2A2 through transition state TS2A2. In TS2A2, the bond length and the charge density at the bond-forming critical point of C1-C2 are 0.2345 nm and 0.0618 a.u., respectively and the activation energy is 36.51 kJ mol^{-1}. IM2A2 forms IM2B2 and R4 directly. The mechanism

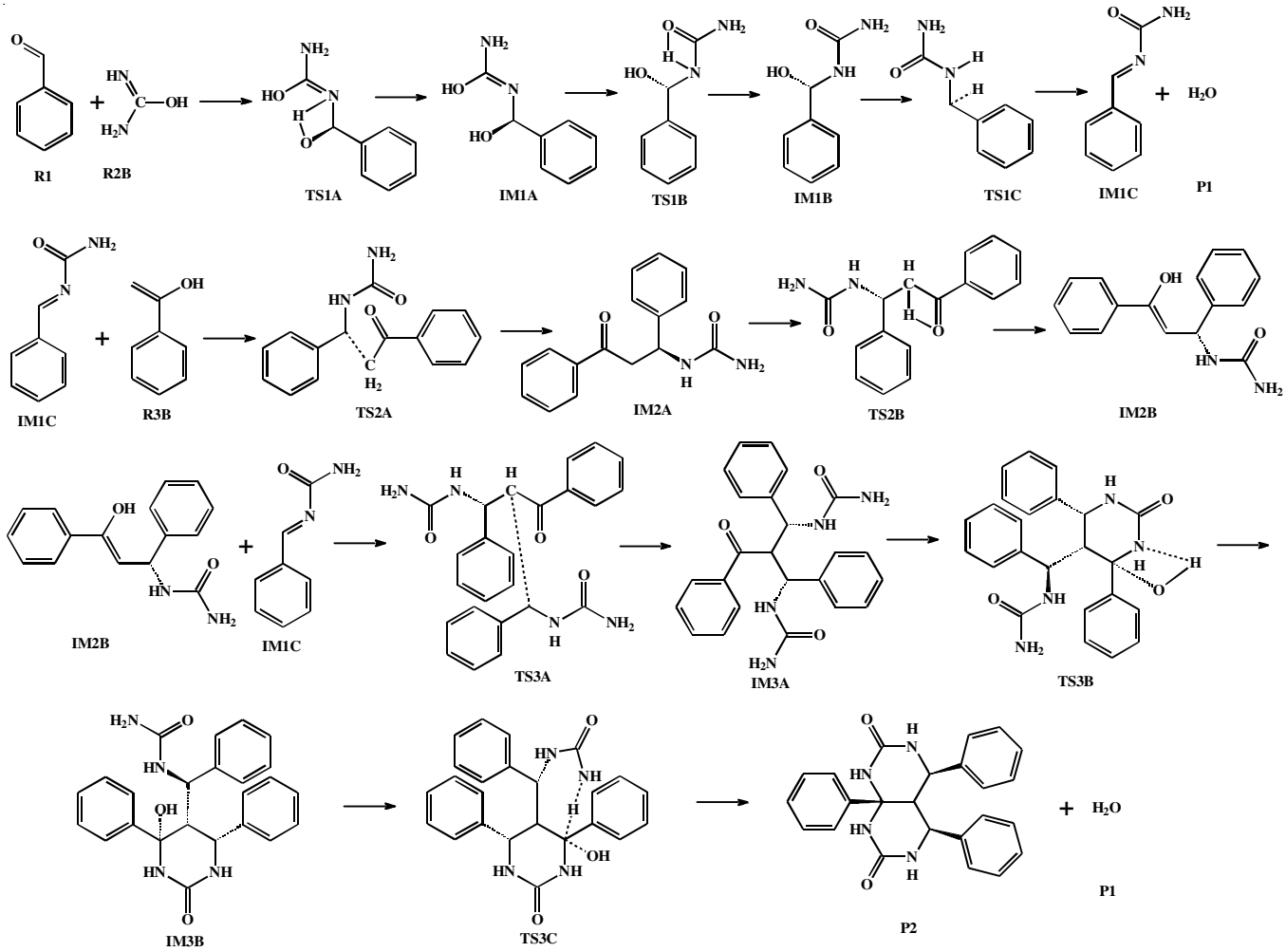

Fig. 4. Mechanism of the reaction with no catalyst

of the reaction is: IM1C2 + R3B → TS2A2 → IM2A2 → IM2B2 + H^+.

IM2B2 reacts with IM1C2 to form IM3A2 through transition state TS3A2. In TS3A2, the bond length and the charge density at the bond-forming critical point of C1-C2 are 0.2213 nm and 0.0568 a.u., respectively and the activation energy is 8.53 kJ mol^{-1}. IM3A2 then forms intermediate IM3B2 through transition state TS3B2. This is a closing the ring processes. In TS3B2, the bond length and the charge density at the bond-forming critical point of N1-C2 are 0.2174 nm and 0.0554 a.u., respectively and the activation energy is 123.31 kJ mol^{-1}. IM3B2 forms intermediate IM3C2 and P1 through transition state TS3C2. This is a concerted reaction process with transferring the hydrogen atom and dehydration process. In TS3C2, the bond length and the charge density at bond-forming critical point of N1–H2 are 0.1343 nm and 0.1300 a.u., respectively and those of H2–O3 are 0.1239 nm and 0.1510 a.u., respectively and the activation energy is 86.78 kJ mol^{-1}. IM3C2 then forms intermediate IM3D2 through transition state TS3D2. In TS3D2, the bond length and the

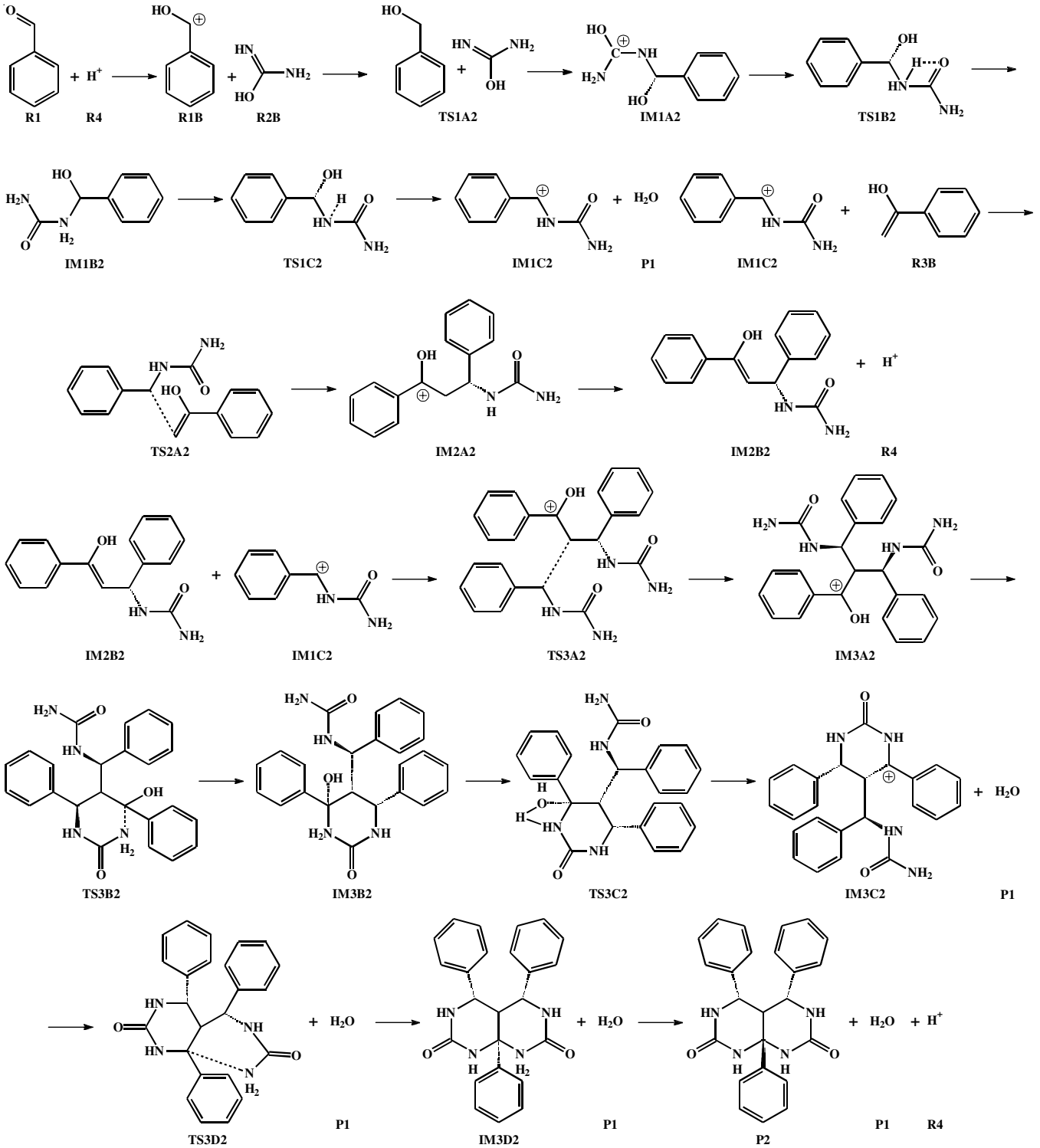

Fig. 5. Mechanism of the reaction with catalyst protonic acid

charge density at the bond-forming critical point of C1-N2 are 0.1943 nm and 0.0902 a.u., respectively and the activation energy is 119.56 kJ mol^{-1}. IM3D2 forms P2 and R4 directly. The mechanism of the reaction is: IM2B2 + IM1C2 → TS3A2 → IM3A2 → TS3B2 → IM3B2 → TS3C2 → IM3C2 + H_2O → TS3D2 + H_2O → IM3D2 + H_2O → P2+ H_2O + H^+.

The overall reaction is: 2R1 + 2R2B + R3B + 2R4 → P2 + 3H_2O + 2R4 and the activation energy of the reaction is 181.26 kJ mol^{-1}. The activation energy of reaction with protonic acid decreased by 104.34 kJ mol^{-1} compared with that of the reaction without protonic acid.

The details of the reaction mechanism of the reaction are shown as Fig. 5.

Conclusion

The microscopic mechanism of reaction among benzaldehyde, urea and acetophenone for the synthesis of (4R,5S,8as)-4,5,8a-triphenylhexahydropyrimido[4,5-d]pyrimidine-2,7(1*H*,3*H*)-dione catalyzed by protonic acid and without protonic acid was investigated by DFT. At the same time, characteristic of catalyst protonic acid was investigated. The following was shown: (1) Protonic acid is an effective catalyst in the synthesis of (4R,5S,8as)-4,5,8a-triphenylhexahydropyrimido[4,5-d]pyrimidine-2,7(1*H*,3*H*)-dione from benzaldehyde, urea and acetophenone. (2) The activation energy with protonic acid decreased by 104.34 kJ mol^{-1} compared with that of the reaction without it. (3) The mechanism of reaction with catalyst protonic acid differs from that of without it. (4) It is identical with Rovnyak *et al*. [15] conclusions and the mechanism of the reaction is the same as that of Biginelli and other authors [1-5].

ACKNOWLEDGEMENTS

The authors thank the Scientific Research Foundation of the Science & Technology Bureau of Dahou for financial support [2013(5) and KJJ2015002].

REFERENCES

1. P. Biginelli, *Ber. Dtsch. Chem. Ges.*, **24**, 1317 (1891).
2. A. Klages and E. Knoevenagel, *Ber. Dtsch. Chem. Ges.*, **26**, 447 (1893).
3. C.O. Kappe, *Bioorg. Med. Chem. Lett.*, **10**, 49 (2000).
4. X.H. Chen, X.Y. Xu, H. Liu, L.F. Cun and L.Z. Gong, *J. Am. Chem. Soc.*, **128**, 14802 (2006).
5. V. Polshettiwar and R.S. Varma, *Tetrahedron Lett.*, **48**, 7343 (2007).
6. L.Z. Gong, X.H. Chen and X.Y. Xu, *Chem. Eur. J.*, **13**, 8920 (2007).
7. N. Ahmed and J.E. van Lier, *Tetrahedron Lett.*, **48**, 5407 (2007).
8. A. Debache, M. Amimour, A. Belfaitah, S. Rhouati and B. Carboni, *Tetrahedron Lett.*, **49**, 6119 (2008).
9. R. Wang and Z.Q. Liu, *J. Org. Chem.*, **77**, 3952 (2012).
10. J.H. Clark, D.J. Macquarrie and J. Sherwood, *Chem. Eur. J.*, **19**, 5174 (2013).
11. I. Sehout, R. Boulcina, B. Boumoud, F. Berree, B. Carboni and A. Debache, *Lett. Org. Chem.*, **10**, 463 (2013).
12. H.G.O. Alvim, T.B. de Lima, H.C.B. de Oliveira, F.C. Gozzo, J.L. de Macedo, P.V. Abdelnur, W.A. Silva and B.A.D. Neto, *ACS Catalysis*, **3**, 1420 (2013).
13. S.R. Alapati, P.K. Pullela, P. Rangappa and V. Pillarisetti, Substituted Dihydropyrimidines, Dihydropyrimidones and Dihydropyrimidine-thiones as Calcium Channel Blockers, US Patent, US7687511 B2 (2010).
14. K.S. Atwal, B.N. Swanson, S.E. Unger, D.M. Floyd, S. Moreland, A. Hedberg and B.C. O'Reilly, *J. Med. Chem.*, **34**, 806 (1991).
15. G.C. Rovnyak, K.S. Atwal, A. Hedberg, S.D. Kimball, S. Moreland, J.Z. Gougoutas, B.C. O'Reilly, J. Schwartz and M.F. Malley, *J. Med. Chem.*, **35**, 3254 (1992).
16. G.J. Grover, S. Dzwonczyk, D.M. McMullen, D.E. Normandin, C.S. Parham, P.G. Sleph and S. Moreland, *J. Cardiovasc. Pharmacol.*, **26**, 289 (1995).
17. S. Putatunda, S. Chakraborty, S. Ghosh, P. Nandi, S. Chakraborty, P.C. Sen and A. Chakraborty, *Eur. J. Med. Chem.*, **54**, 223 (2012).
18. S.S. Kshirsagar and P. Shanmugasundaram, *Int. J. Chem. Technol. Res.*, **5**, 2899 (2013).
19. Y.M. Litvinov, A.A. Shestopalov, L.A. Rodinovskaya and A.M. Shestopalov, *J. Comb. Chem.*, **11**, 914 (2009).
20. Z.L. Shen, X.P. Xu and S.J. Ji, *J. Org. Chem.*, **75**, 1162 (2010).
21. F. Shi, R.H. Jia, X.J. Zhang, S.J. Tu, S. Yan, Y. Zhang, B. Jiang, J.Y. Zhang and C.S. Yao, *Synthesis*, **18**, 2782 (2007).
22. R.F.W. Bader, Atoms in Molecules: A Quantum Theory; Clarendon: Oxford, U.K. (1990).
23. P.L. Prpelier, Atoms in Molecules: An Introduction; Pearson Education: Halow, U.K. (1999).
24. M. Takahashi, S. Tsutsui, K. Sakamoto, M. Kira, T. Müller and Y. Apeloig, *J. Am. Chem. Soc.*, **123**, 347 (2001).
25. M.J. Frisch, G.W. Trucks, H.B. Schlegel, G.E. Scuseria, M.A. Robb, J.R. Cheeseman, J.A. Montgomery Jr., T. Vreven, K.N. Kudin, J.C. Burant, J.M. Millam, S.S. Iyengar, J. Tomasi, V. Barone, B. Mennucci, M. Cossi, G. Scalmani, N. Rega, G.A. Petersson, H. Nakatsuji, M. Hada, M. Ehara, K. Toyota, R. Fukuda, J. Hasegawa, M. Ishida, T. Nakajima, Y. Honda, O. Kitao, H. Nakai, M. Klene, X. Li, J.E. Knox, H.P. Hratchian, J.B. Cross, C. Adamo, J. Jaramillo, R. Gomperts, R.E. Stratmann, O. Yazyev, A.J. Austin, R. Cammi, C. Pomelli, J.W. Ochterski, P.Y. Ayala, K. Morokuma, G.A. Voth, P. Salvador, J.J. Dannenberg, V.G. Zakrzewski, S. Dapprich, A.D. Daniels, M.C. Strain, O. Farkas, D.K. Malick, A.D. Rabuck, K. Raghavachari, J.B. Foresman, J.V. Ortiz, Q. Cui, A.G. Baboul, S. Clifford, J. Cioslowski, B.B. Stefanov, G. Liu, A. Liashenko, P. Piskorz, I. Komaromi, R.L. Martin, D.J. Fox, T. Keith, M.A. Al-Laham, C.Y. Peng, A. Nanayakkara, M. Challacombe, P.M.W. Gill, B. Johnson, W. Chen, M.W. Wong, C. Gonzalez and J.A. Pople, Gaussian, Inc.: Pittsburgh, PA (2003).